# Semiconductor saturable absorber mirror mode-locked Yb:YAP laser

Zhang-Lang Lin, Wen-Ze Xue, Huang-Jun Zeng, Ge Zhang, Yongguang Zhao, Xiaodong Xu, Jun Xu, Pavel Loiko, Xavier Mateos, Haifeng Lin, et al.

Research Article | Vol. 30, No. 18 / 29 Aug 2022 / Optics Express 31986
Optics EXPRESS

# Semiconductor saturable absorber mirror mode-locked Yb:YAP laser

ZHANG-LANG LIN,[1] WEN-ZE XUE,[1] HUANG-JUN ZENG,[1] GE ZHANG,[1] YONGGUANG ZHAO,[2] XIAODONG XU,[2,8] JUN XU,[3] PAVEL LOIKO,[4] XAVIER MATEOS,[5] HAIFENG LIN,[6] VALENTIN PETROV,[7] LI WANG,[7,*] AND WEIDONG CHEN[1,7]

[1]*Fujian Institute of Research on the Structure of Matter, Chinese Academy of Sciences, 350002 Fuzhou, China*
[2]*Jiangsu Key Laboratory of Advanced Laser Materials and Devices, Jiangsu Normal University, 221116 Xuzhou, China*
[3]*School of Physics Science and Engineering, Institute for Advanced Study, Tongji University, 200092 Shanghai, China*
[4]*Centre de Recherche sur les Ions, les Matériaux et la Photonique (CIMAP), UMR 6252 CEA-CNRS-ENSICAEN, Université de Caen, 6 Boulevard Maréchal Juin, 14050 Caen Cedex 4, France*
[5]*Universitat Rovira i Virgili, URV, Física i Cristal·lografia de Materials, (FiCMA)- Marcel·lí Domingo 1, 43007 Tarragona, Spain*
[6]*College of Physics and Optoelectronic Engineering, Shenzhen University, 518118 Shenzhen, China*
[7]*Max Born Institute for Nonlinear Optics and Short Pulse Spectroscopy, Max-Born-Str. 2a, 12489 Berlin, Germany*
[8]*xdxu79@jsnu.edu.cn*
[*]*Li.Wang@mbi-berlin.de*

**Abstract:** We report on sub-30 fs pulse generation from a semiconductor saturable absorber mirror mode-locked Yb:YAP laser. Pumping by a spatially single-mode Yb fiber laser at 979 nm, soliton pulses as short as 29 fs were generated at 1091 nm with an average output power of 156 mW and a pulse repetition rate of 85.1 MHz. The maximum output power of the mode-locked Yb:YAP laser amounted to 320 mW for slightly longer pulses (32 fs) at an incident pump power of 1.52 W, corresponding to a peak power of 103 kW and an optical efficiency of 20.5%. To the best of our knowledge, this result represents the shortest pulses ever achieved from any solid-state Yb laser mode-locked by a slow, i.e., physical saturable absorber.



## 1. Introduction

Mode-locked (ML) solid-state lasers based on Yb dopant, emitting in the 1-μm spectral range represent currently a "work horse" providing ultrashort pulses with high average/peak power for multiple applications. $Yb^{3+}$-doped laser materials feature i) very simple two manifold electronic level structure which allows one to avoid most of the parasitic effects including excited-state absorption, energy-transfer upconversion and cross-relaxation, ii) very low quantum defect (~7%) arising from the in-band pumping scheme which is beneficial for reaching high laser efficiencies and weak heat load, iii) broad emission bands supporting ultrashort pulse generation down to below 30 fs, and iv) broad absorption bands well matching the emission of commercial high-power InGaAs laser diodes and thus supporting power scalable operation.

$Yb^{3+}$-doped structurally disordered crystals featuring a significant inhomogeneous spectral line broadening (a "glassy-like" spectroscopic behavior: with extremely broad, flat and smooth gain profiles) are currently widely used to generate sub-40 fs pulses from ML Yb lasers [1–17]. For lasers based on such materials, even sub-20 fs pulses could be directly generated via Kerr-lens mode-locking (KLM) as recently demonstrated with $Yb^{3+}$-doped calcium rare-earth aluminate

#464815 https://doi.org/10.1364/OE.464815
Journal © 2022 Received 7 Jun 2022; revised 8 Aug 2022; accepted 9 Aug 2022; published 17 Aug 2022

Optics EXPRESS

crystals, e.g., Yb:$CaGdAlO_4$ [18] and Yb:$CaYAlO_4$ [19]. However, using structurally disordered crystals as a gain medium will inevitably lead to a certain trade-off between the achievable pulse duration, maximum average output power as well as laser efficiency, which is due to the reduced thermal conductivity of such host materials and the lower peak emission cross-section of the dopant $Yb^{3+}$ dopant ions. Until now, structurally ordered $Yb^{3+}$-doped crystals have never outperformed the disordered ones in terms of generating the shortest pulses from ML lasers at ~1 μm.

The KLM technique is normally adopted for utilizing the maximum available gain bandwidth due to its quasi-instantaneous response acting as an artificial "fast" saturable absorber (SA). A diode-pumped Yb:$Y_3Al_5O_{12}$ (Yb:YAG) laser delivered 35 fs pulses at 1060 nm with an average output power of 107 mW via soft-aperture KLM [20]. Employing a distributed Kerr-medium, soliton pulses as short as 27 fs were generated from a KLM thin-disk Yb:YAG laser at 1028 nm with an average output power of 3.3 W at an incident pump power of 315 W, corresponding to a relatively low laser efficiency of 1.1% [21]. Although using the KLM technique has the advantage of generating shorter pulses compared to a physical "slow" SA, it imposes tight constraints on the cavity alignment towards its stability limit and is prone to instabilities, which set a limit for a wide range of commercial applications. Alternatively, mode-locking with a physical "slow" SA, e.g., a SEmiconductor Saturable Absorber Mirror (SESAM), is a well-established technique for generating femtosecond pulses from solid-state lasers [22–24]. Without KLM, the shortest pulses generated from a diode-pumped SESAM ML Yb:$LiYF_4$ laser at 1050.8 nm had a duration of 40 fs for an average output power of 263 mW [25]. No sub-30 fs pulse generation from any "slow" SA ML Yb laser based on an $Yb^{3+}$-doped structurally ordered laser crystal has been demonstrated so far.

$Yb^{3+}$-doped yttrium orthoaluminate, i.e., Yb:$YAlO_3$ (abbreviated Yb:YAP), represents one of the most promising structurally ordered crystals favoring high-power laser applications. It crystallizes in the same binary system ($Y_2O_3$ – $Al_2O_3$ [26]) as the well-known YAG crystal while belonging to the orthorhombic class with a perovskite-type ($CaTiO_3$) structure (sp. gr. $D_{2h}^{16}$ – *Pnma*) and lattice constants of $a = 5.330$ Å, $b = 7.375$ Å and $c = 5.180$ Å (for undoped crystal [27]). YAP is optically biaxial [28] and its intrinsic birefringence and the polarized spectroscopic properties of the dopant ion result in a linearly polarized emission with weak depolarization losses during high power laser operation [29]. This crystal also provides high thermal conductivity even for high doping levels, $\kappa_a = 7.1$, $\kappa_b = 8.3$ and $\kappa_c = 7.6$ $Wm^{-1}K^{-1}$ (values along the crystallographic axes for 5 at.% $Yb^{3+}$ doping) [30]. Finally, YAP can be easily grown in large volume by the Bridgman or Czochralski (Cz) methods with high $Yb^{3+}$ concentrations (up to ~10 at.%) [31]. Given the combination of good thermo-mechanical and spectroscopic properties of the Yb:YAP crystal [32,33], it has attracted attention for high-power femtosecond pulse generation from ML lasers pumped by commercially available InGaAs laser diodes. In the first demonstration of a SESAM ML Yb:YAP laser, 225 fs pulses at 1041 nm were generated with an average output power of 0.8 W [34]. Subsequently, an average output power of 4 W was achieved from a diode-pumped SESAM ML Yb:YAP laser at 1009.7 nm corresponding to a pulse duration of 140 fs [35]. Very recently, we demonstrated sub-50 fs soliton pulse generation from a diode-pumped SESAM ML laser using an $Yb^{3+}$-doped yttrium-gadolinium "mixed" orthoaluminate crystal, i.e., Yb:$Y_{1-x}Gd_xAlO_3$ or Yb:(Y,Gd)$AlO_3$, which benefited from the compositional disorder [36].

In the present work, we exploit an $Yb^{3+}$-doped YAP crystal for generating sub-30 fs pulses from a passively ML laser. Implementing a SESAM as a SA, the Yb:YAP laser emitted soliton pulses as short as 29 fs with a spectral bandwidth exceeding the available gain profile, which indicates the ML laser is operating in a self-phase modulation (SPM) spectral broadening regime where soliton mode-locking dominates the pulse shaping and it is stabilized by the SESAM.

Optics EXPRESS

## 2. Experimental setup

### 2.1. Spectroscopic properties of Yb:YAP

A high-quality Yb:YAP crystal was grown along the [101] direction by the Czochralski method [37–39]. The actual $Yb^{3+}$ doping concentration was measured by the ICP-MS method to be $9.86 \times 10^{20}$ $cm^{-3}$, corresponding to 5 at.%. This doping level is close to the optimum one for $Yb^{3+}$ ions in $YAlO_3$ as concluded by Boulon *et al.* based on the analysis of luminescence quenching for this material [29]. For orthorhombic crystals the optical indicatrix axes coincide with the crystallographic ones. Thus, the spectral properties of Yb:YAP were characterized for the three principal light polarizations, $\boldsymbol{E} \parallel \boldsymbol{a}$, $\boldsymbol{b}$ and $\boldsymbol{c}$ (sp. gr. $P_{nma}$).

The room temperature (RT) polarized absorption cross-section ($\sigma_{abs}$) spectra of the Yb:YAP crystal are shown in Fig. 1(a). This material exhibits a strong polarization anisotropy of optical absorption. The maximum $\sigma_{abs}$ reaches $4.15 \times 10^{-20}$ $cm^2$ at 977.7 nm (zero phonon line, ZPL) and the corresponding absorption bandwidth (determined at full width at half maximum, FWHM) reaches 6.1 nm for light polarization $\boldsymbol{E} \parallel \boldsymbol{b}$. For other two polarizations, the absorption is much weaker, namely $\sigma_{abs}$ reaches $0.94\times 10^{-20}$ $cm^2$ at 977.8 nm ($\boldsymbol{E} \parallel \boldsymbol{a}$) and $0.60\times 10^{-20}$ $cm^2$ at 978.2 nm ($\boldsymbol{E} \parallel \boldsymbol{c}$). The relatively broad ZPL releases the limitations for pumping the Yb:YAP crystal with high-power InGaAs laser diodes related to the possible temperature drift of the diode wavelength.

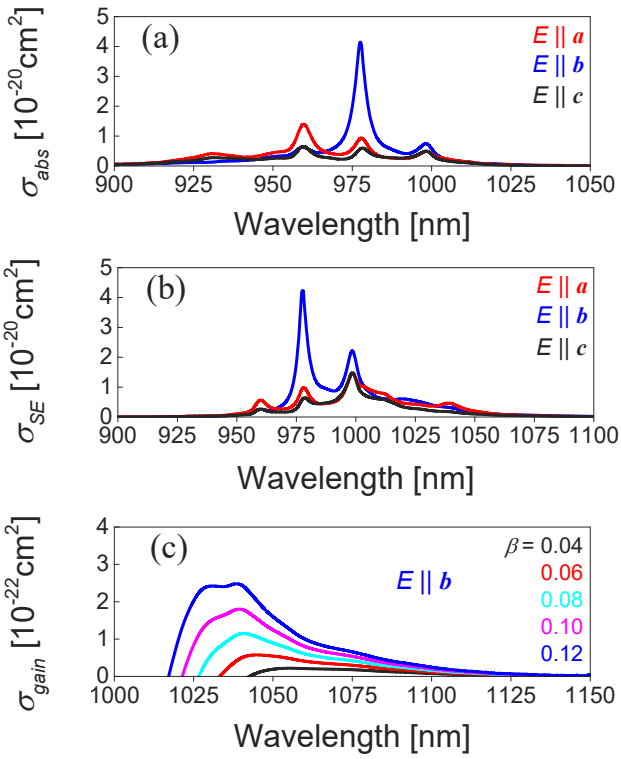


**Fig. 1.** Room-temperature polarized spectroscopy of $Yb^{3+}$ ions in the YAP crystal for light polarizations $\boldsymbol{E} \parallel \boldsymbol{a}, \boldsymbol{b}$ and $\boldsymbol{c}$: (a) absorption ($\sigma_{abs}$) and (b) stimulated-emission (SE, $\sigma_{SE}$) cross-sections; (c) gain cross-sections, $\sigma_{gain} = \beta\sigma_{SE} - (1 - \beta)\sigma_{abs}$ for different inversion ratios $\beta$, $\boldsymbol{E} \parallel \boldsymbol{b}$.

Optics EXPRESS

The stimulated emission (SE) cross-sections ($\sigma_{SE}$) were calculated using a combination of the reciprocity method (RM) and the Füchtbauer–Ladenburg (F-L) formula. For the RM, we have used the experimental crystal-field splitting determined by Boulon *et al.* at RT: $^2F_{7/2}$ = (0, 209, 341, 590) cm$^{-1}$ and $^2F_{5/2}$ = (10220, 10410, 10730) cm$^{-1}$ [26]. For the F-L formula, we have used polarized luminescence spectra measured in this work and a radiative lifetime of the $^2F_{5/2}$ excited-state reported in [26], $\tau_{rad}$ = 0.60 ms. The mean refractive index of YAP, $<n>$ = 1.92 at 1.05 µm, was taken from [25]. The polarized SE cross-section spectra are shown in Fig. 1(b). The emission spectra of $Yb^{3+}$ ions in YAP are strongly polarized. Despite the moderate total Stark splitting of the ground-state, $\Delta E(^2F_{7/2})$ = 590 cm$^{-1}$, the spectra extend up to at least 1.15 µm owing to a strong electron-phonon interaction in this material. For light polarization $\boldsymbol{E} \parallel \boldsymbol{b}$, the maximum $\sigma_{SE}$ is $4.22 \times 10^{-20}$ cm$^2$ at 977.7 nm (ZPL) and at longer wavelengths where the laser operation is expected, $\sigma_{SE}$ is $0.61 \times 10^{-20}$ cm$^2$ at ~1020 nm.

According to the quasi-three-level nature of the Yb laser, the gain cross-sections, $\sigma_{gain} = \beta\sigma_{SE} - (1-\beta)\sigma_{abs}$, were calculated, where $\beta = N_2/N_{Yb}$ is the inversion ratio and $N_2$ is the population of the upper laser level ($^2F_{5/2}$). The polarized gain profiles for light polarization $\boldsymbol{E} \parallel \boldsymbol{b}$ for small inversion ratios in the range of 0.04 – 0.12 are shown in Fig. 1(c). For very small $\beta$ = 0.04, the gain bandwidth (FWHM) is as broad as 46 nm with a maximum at ~1055 nm and for higher $\beta$ = 0.12, it is reduced to 34 nm corresponding to a blue-shift of the peak wavelength to ~1039 nm, indicating that Yb:YAP can naturally support broadly tunable operation and sub-50 fs pulse generation from ML lasers. Note that the flat and broad gain extending until 1.15 µm is mainly due to the long-wave multiphonon-assisted (vibronic) emission.

### 2.2. Laser setup

The experimental setup of the Yb:YAP laser is shown in Fig. 2. A linear X-shaped astigmatically compensated resonator was employed for evaluating the laser performance of the Yb:YAP crystal both in the continuous-wave (CW) and ML regimes. A CW Yb fiber laser emitting linearly polarized radiation at 979 nm was used as a pump source. It provided a nearly diffraction-limited spatial intensity profile with a beam propagation factor ($M^2$) of ~1.04 and an emission bandwidth of ~0.1 nm (FWHM). A 5 at.% Yb:YAP laser element was cut from the as-grown bulk crystal for light propagation along the crystallographic $\boldsymbol{c}$-axis ($\boldsymbol{c}$-cut) having an aperture of 3 ($\boldsymbol{a}$) mm × 3 ($\boldsymbol{b}$) mm and a thickness of 3 mm. It was double-side polished with laser quality and good parallelism. The uncoated sample was mounted in a water-cooled copper holder kept at 19°C and placed at Brewster's angle between the two concave folding mirrors $M_1$ and $M_2$ (radius of curvature, RoC = -100 mm) with the Brewster minimum loss condition fulfilled for both the pump and laser wavelengths. This orientation of the laser crystal was selected to ensure high pump absorption at ~979 nm for light polarization $\boldsymbol{E} \parallel \boldsymbol{b}$. A spherical focusing lens L (focal length: $f$ = 75 mm) was

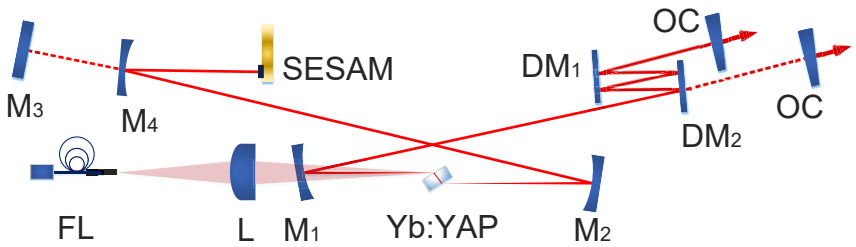


**Fig. 2.** Experimental setup of the Yb:YAP laser. FL: Yb fiber laser emitting at 979 nm; L: spherical lens; $M_1$, $M_2$ and $M_4$: concave mirrors (RoC = -100 mm); $M_3$: flat rear mirror for CW laser operation; $DM_1$ and $DM_2$: flat dispersive mirrors; OC: output coupler; SESAM: SEmiconductor Saturable Absorber Mirror.

Optics EXPRESS

employed to focus the pump beam into the crystal through the $M_1$ dichroic mirror yielding a beam waist (radius) of 15.4 μm × 28.6 μm in the sagittal and tangential planes, respectively.

## 3. Continuous-wave laser operation

For the CW laser operation, a four-mirror cavity was used. One cavity arm was terminated by a flat rear mirror $M_3$ and the other arm – by a flat output coupler (OC) having a transmission at the laser wavelength $T_{OC}$ in the range 1% - 10%. The cavity mode size inside the laser crystal was estimated by the ABCD formalism yielding a waist radius of 22.5 μm × 42.3 μm in the sagittal and the tangential planes, respectively. The physical cavity length of the Yb:YAP laser in the CW regime was 1.3 m. The measured single-pass pump absorption under lasing conditions was almost independent of the transmission of the OC ranging from 98.9% to 99.5%. The maximum output power of 3.91 W was achieved with a 7.5% OC at an absorbed pump power of 5.89 W and a laser threshold of 438 mW. This corresponds to an optical efficiency of 66.4% and a slope efficiency of 71.5%, see Fig. 3(a). A slightly higher slope efficiency of 72.7% was obtained with a 10% OC for an output power of 3.86 W at an absorbed power of 5.9 W. The laser threshold gradually increased with the transmission of the OC, from 276 mW ($T_{OC}$ = 1%) to 513 mW ($T_{OC}$ = 10%). The laser emission wavelength in the CW regime experienced a monotonic blue-shift with increasing the transmission of the OC in the range of 1039.7 – 1062.3 nm, as shown in Fig. 3(b). This behavior is typical for quasi-three-level Yb lasers with inherent reabsorption at the laser wavelength. The laser emission was linearly polarized ($\boldsymbol{E} \parallel \boldsymbol{b}$). While this polarization is expected to be also naturally selected, in the present laser it was imposed by the Brewster condition for the active element.

The Caird analysis was applied by fitting the measured laser slope efficiency as a function of the output coupler reflectivity, $R_{OC} = 1 - T_{OC}$ [40]. The total round-trip cavity losses δ (reabsorption losses excluded), as well as the intrinsic slope efficiency $\eta_0$ (accounting for the

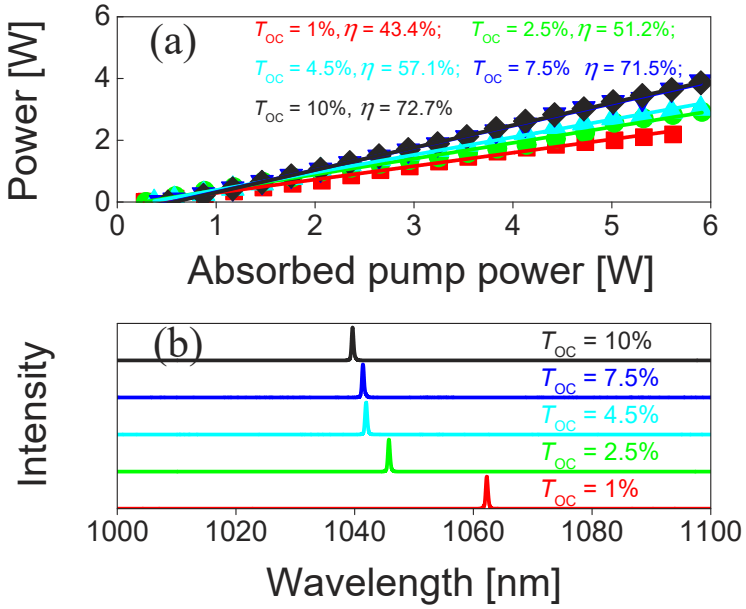


**Fig. 3.** CW Yb:YAP laser: (a) input-output dependences for different OCs, $\eta$ – slope efficiency; (b) typical spectra of laser emission, $\boldsymbol{E} \parallel \boldsymbol{b}$.

Optics EXPRESS

mode-matching and the quantum efficiencies) were estimated yielding $\delta = 0.9\% \pm 0.4\%$ and $\eta_0 = 81.9\%$, respectively, as shown in Fig. 4(a). The wavelength tuning of the CW Yb:YAP laser was studied by inserting a 2-mm thick quartz plate acting as a Lyot filter close to the OC ($T_{OC} = 1\%$) at an incident pump power of 2.6 W. The Lyot filter was aligned at Brewster's angle for the oscillating polarization. The laser wavelength was continuously tunable between 1008.4 and 1102.1 nm, i.e., across 93.7 nm at the zero-power-level, see Fig. 4(b).

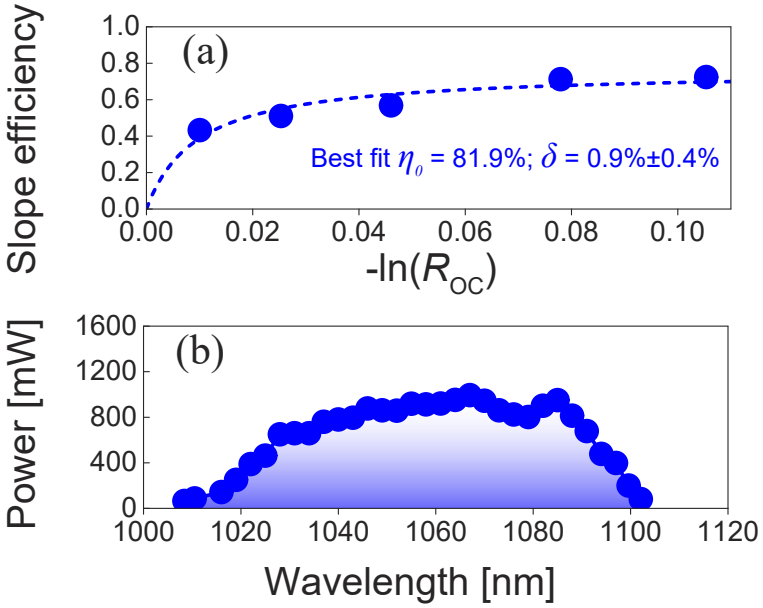


**Fig. 4.** CW Yb:YAP laser: (a) Caird analysis: slope efficiency *vs* $R_{OC} = 1 - T_{OC}$; (b) tuning curve obtained with a Lyot filter and $T_{OC} = 1\%$. The laser polarization is $\boldsymbol{E} \parallel \boldsymbol{b}$.

## 4. Mode-locked laser operation

For ML operation, the flat rear mirror $M_3$ was substituted by a curved mirror $M_4$ (RoC = -100 mm) in order to create a second beam waist on the SESAM for efficient saturation, with a calculated beam radius of ~60 µm. A commercial SESAM (BATOP, GmbH) with a modulation depth of 0.6%, a recovery time of ~1 ps, a non-saturable loss of ~0.4% and a high reflection band ranging from 1000 nm – 1070 nm was implemented to start and stabilize the ML operation. The intracavity group delay dispersion (GDD) was managed by implementing two flat dispersive mirrors (DMs) characterized by the following GDD per bounce: $DM_1 = -200$ fs$^2$ and $DM_2 = -100$ fs$^2$. The resulting round-trip negative GDD amounted to -1200 fs$^2$ in order to compensate the materials dispersion and to balance the SPM induced by the Kerr nonlinearity of the crystal. The round-trip material dispersion due to the 3-mm thick Yb:YAP crystal was estimated from the dispersion curve [28] to be ~+534 fs$^2$ at 1080 nm. The physical cavity length of the ML laser was 1.76 m which corresponded to a pulse repetition rate of ~85 MHz.

The Yb:YAP laser was initially ML with an intermediate 2.5% OC. After careful cavity alignment, stable and self-starting ML operation was readily achieved. The measured optical spectrum of the laser pulses plotted both in linear and logarithmic scales is shown in Fig. 5(a). It has an emission bandwidth (FWHM) of 41.4 nm at a central wavelength of 1075 nm by assuming a sech$^2$-shaped spectral profile. The recorded intensity autocorrelation trace was almost perfectly fitted with a sech$^2$-shaped temporal pulse profile giving a pulse duration (FWHM) of 32 fs

Optics EXPRESS

corresponding to a time-bandwidth-product (TBP) of 0.344, see Fig. 5(b). An average output power of 320 mW was obtained at an incident pump power of 1.56 W, corresponding to a laser efficiency of 20.5% and a peak power of 103 kW. In this case, the on-axis peak intensity in the Yb:YAP crystal amounted to 193 GW/cm$^2$. The inset in Fig. 5(b) shows the measured intensity autocorrelation trace on a long-time span of 50 ps indicating single-pulse CW-ML operation free of multiple pulse instabilities.

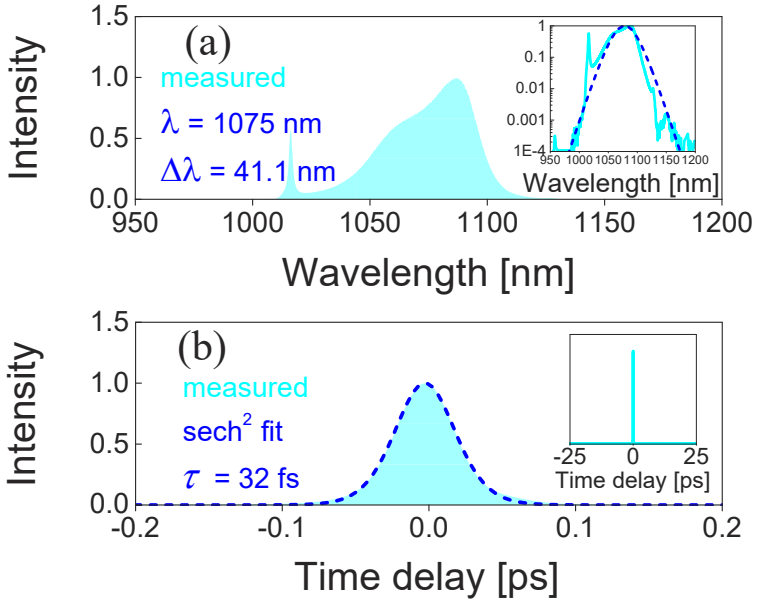


**Fig. 5.** SESAM ML Yb:YAP laser with $T_{OC} = 2.5\%$. (a) Optical spectrum, *Inset*: spectral profile in logarithmic scale with a sech$^2$ fit; (b) background-free autocorrelation trace. *Inset*: autocorrelation trace measured on a time span of 50 ps.

A radio-frequency (RF) spectrum analyzer was used for confirming the stability of the ML operation. A relatively high extinction ratio of >80 dBc above the noise level for the fundamental beat note at 85.3 MHz in combination with the uniform harmonics recorded on a 1-GHz frequency span are evidence for highly stable ML operation without any Q-switching or multi-pulsing instabilities, see Fig. 6.

It is well known from passive mode-locking analytical theory that the pulse duration can be shortened by applying lower transmission of the output coupler at the expense of the average output power. The shortest pulses with ultimate stability were achieved with yet smaller 1% OC. The measured laser spectrum, plotted again both in linear and logarithmic scales, is shown in Fig. 7(a). Assuming a sech$^2$-shaped spectral profile [see also the inset in Fig. 7(a)], the self-starting ML Yb:YAP laser delivered pulses having a spectral bandwidth of 47 nm at 1091 nm, i.e., being notably broader that the gain bandwidth of the laser crystal [~34 nm, cf. Fig. 1(b)], see Fig. 7(a).

Figure 7(b) shows the recorded background-free intensity autocorrelation trace for the shortest pulses. The curve is fitted with a sech$^2$-shaped temporal profile, yielding an estimation of 29 fs (~8 optical cycles) for the pulse duration. This could be confirmed by a fringe-resolved interferometric autocorrelation measurement, see Fig. 7(c). The corresponding TBP was 0.343 which is slightly above the Fourier-transform-limit. The inset in Fig. 7(b) shows the measured background-free intensity autocorrelation trace on a long-time span of 50 ps indicating single-pulse CW-ML operation free of multiple pulse instabilities. The average output power for the shortest pulses

Optics EXPRESS

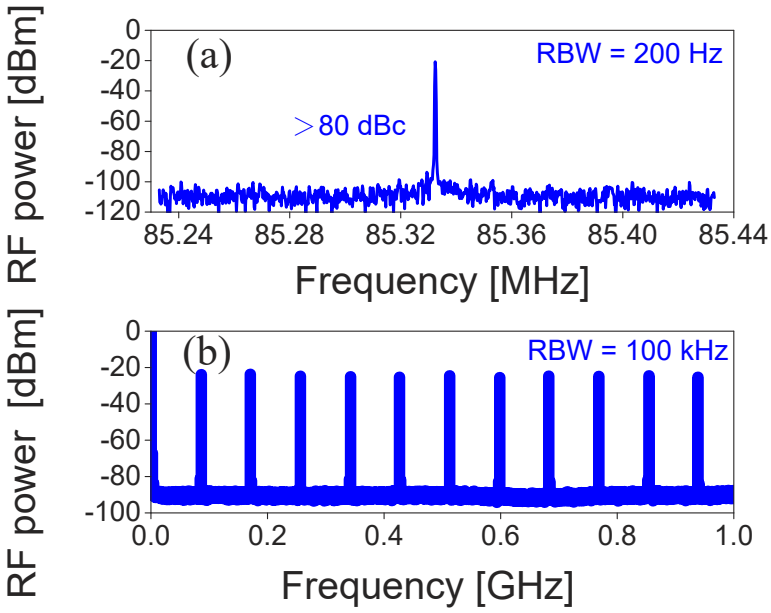


**Fig. 6.** RF spectra of the SESAM ML Yb:YAP laser with $T_{OC} = 2.5\%$: (a) fundamental beat note at 85.32 MHz recorded with a resolution bandwidth (RBW) of 200 Hz, and (b) harmonics on a 1-GHz frequency span recorded with a RBW of 100 kHz.

amounted to 156 mW at an incident pump power of 1.52 W, corresponding to a laser efficiency of 10.3% and a peak power of 55.6 kW. As already mentioned the spectrum of the ML Yb:YAP laser significantly exceeded in width the calculated gain profile of the laser crystal and clearly extended towards longer wavelengths even beyond 1180 nm where no gain is expected, see Fig. 7(a). Such spectral behavior indicates that the Yb:YAP laser was operating in a regime with strong self-phase modulation leading to substantial spectral broadening. For this OC, the estimated peak on-axis intensity in the crystal amounted to 262 GW/cm$^2$. Recently, Drs *et al.* reported on a Kerr-lens mode-locked Yb:YAG thin-disk laser generating 27 fs pulses at 1028 nm (emission bandwidth: 39.8 nm, notably exceeding the gain bandwidth of ~8 nm in the laser crystal) [21]. The frequencies outside of the gain bandwidth were generated by intracavity SPM inside the Kerr-active medium [41], while the operation in the SPM-broadened regime followed the standard soliton mode-locking scheme.

The RF spectra of the shortest pulses were recorded to verify the ultimate stability of the ML operation in different frequency span ranges, as shown in Fig. 8. The recorded first beat note located at 85.1 MHz exhibited a high extinction ratio of >81 dBc above carrier. The measured uniform harmonics on a 1-GHz frequency span again revealed high stability of the single-pulse ML operation.

In order to confirm the pulse shaping mechanism, far-field beam profiles of the Yb:YAP laser both in the CW and self-starting ML regimes were recorded with an IR camera placed at ~0.7 m away from the OC. It was relatively easy to switch between the ML and CW laser operation regimes by a slight cavity misalignment, see Fig. 9. A slight spatial modification of the far-field beam profile could be observed without a significant beam shrinking. This phenomenon is very similar to the observation in Yb:$SrF_2$ [42], which indicates that the underlying pulse shaping mechanism is soliton mode-locking [43] sustained by the SESAM rather than Kerr-lens mode-locking.

Optics EXPRESS

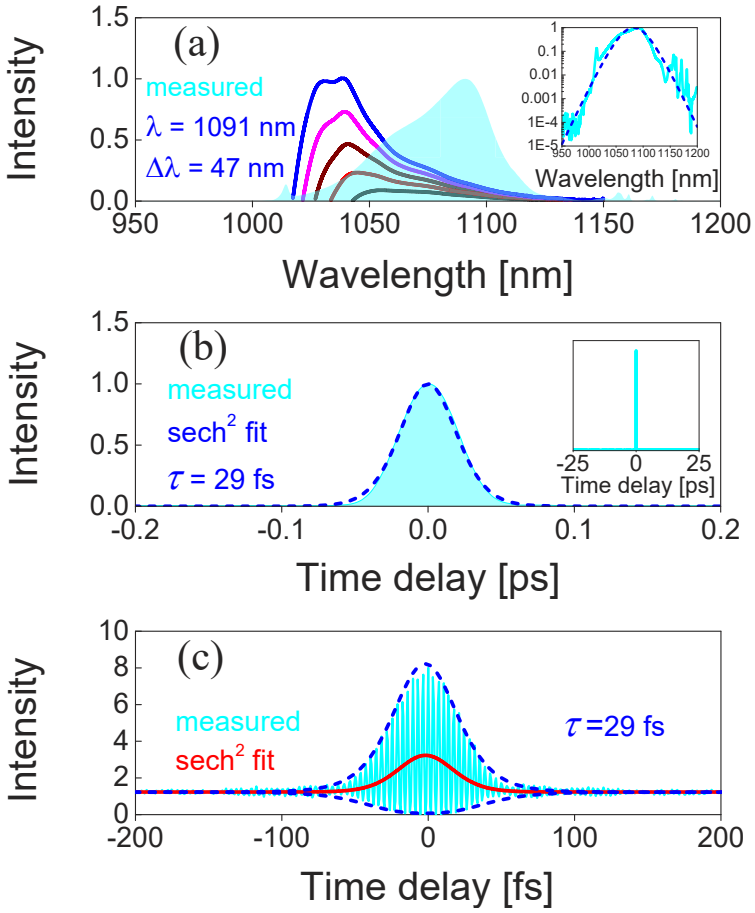


**Fig. 7.** SESAM ML Yb:YAP laser with $T_{OC} = 1\%$. (a) Optical spectrum plotted together with gain profiles (not in scale), with inversion ratios $\beta$ in the range from 0.04 to 0.12 for light polarization $\boldsymbol{E} \parallel \boldsymbol{b}$, *Inset*: spectral profile in logarithmic scale with a $\text{sech}^2$ fit; (b) background free intensity autocorrelation trace. *Inset*: autocorrelation trace on a time span of 50 ps; (c) interferometric autocorrelation trace.

Optics EXPRESS

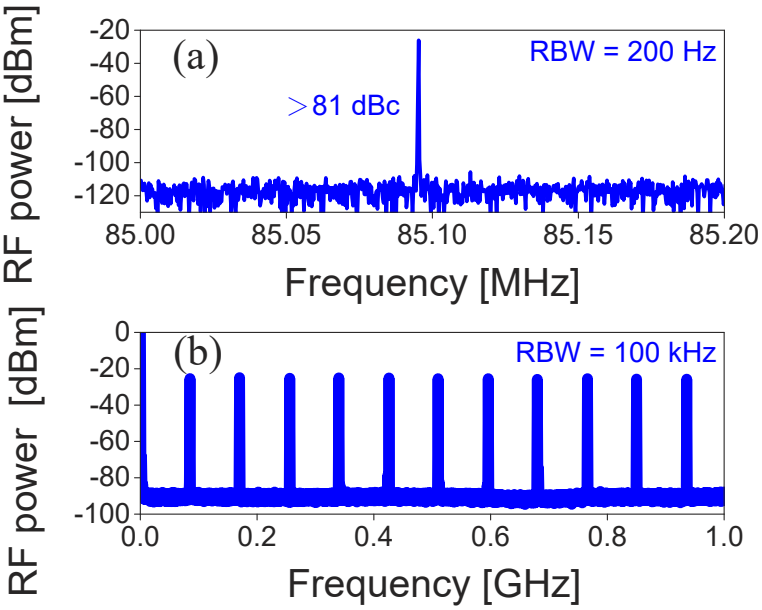


**Fig. 8.** RF spectra of the SESAM ML Yb:YAP laser with $T_{OC} = 1\%$: (a) fundamental beat note at 85.09 MHz recorded with a resolution bandwidth (RBW) of 200 Hz, and (b) harmonics on a 1-GHz frequency span recorded with a RBW of 100 kHz.

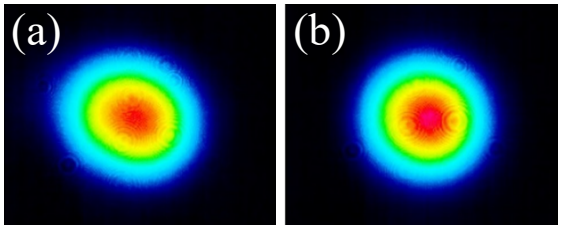


**Fig. 9.** Measured far-field beam profiles of the Yb:YAP laser: (a) CW and (b) ML regimes of operation; $T_{OC} = 1\%$, the laser polarization is horizontal corresponding to $\boldsymbol{E} \,||\, \boldsymbol{b}$.

## 5. Conclusion

To conclude, we report on sub-30 fs pulse generation from a SESAM mode-locked solid-state laser using an $Yb^{3+}$-doped YAP crystal. This result represents the shortest pulse duration ever obtained from any solid-state Yb laser ML with a slow, i.e., physical saturable absorber. Pumping by a high-brightness Yb fiber laser at 979 nm, the SESAM mode-locked Yb:YAP laser delivered soliton pulses as short as 29 fs at a central wavelength of 1091 nm with an average output power of 156 mW at an incident pump power of 1.52 W, corresponding to a laser efficiency of 10.3%. The self-starting ML Yb:YAP laser was operating in the strongly self-phase modulation spectral broadened regime as evidenced by the measured laser spectrum significantly exceeding the available gain profile of the laser crystal, as well as very high peak on-axis intensity in the laser crystal. Our results indicate the potential of Yb:YAP crystals for further power scaling and pulse shortening via the Kerr-lens mode-locking technique.

**Funding.** National Key Research and Development Program of China (2018YFB2201101); National Natural Science Foundation of China (61975208, 61875199, 61905247, 52032009, 61850410533, 62075090, U21A20508); Sino-German Scientist Cooperation and Exchanges Mobility Program (M-0040).

Optics EXPRESS

**Acknowledgment.** Xavier Mateos acknowledges the Serra Húnter program.

**Disclosures.** The authors declare no conflicts of interest.

**Data availability.** Data underlying the results presented in this paper are not publicly available at this time but may be obtained from the authors upon reasonable request.

## References


1. Z. Pan, Z. L. Lin, P. Loiko, G. Zhang, H. J. Zeng, W. Z. Xue, P. Camy, V. Petrov, S. Slimi, X. Mateos, F. Díaz, H. Lin, L. Wang, and W. Chen, "Polarized spectroscopy and diode-pumped laser operation of disordered Yb:$Ca_3Gd_2(BO_3)_4$ crystal," Opt. Mater. Express **12**(2), 673–684 (2022).
2. P. Loiko, J. M. Serres, X. Mateos, X. Xu, J. Xu, V. Jambunathan, P. Navratil, A. Lucianetti, T. Mocek, X. Zhang, U. Griebner, V. Petrov, M. Aguiló, F. Díaz, and A. Major, "Microchip Yb:$CaLnAlO_4$ lasers with up to 91% slope efficiency," Opt. Lett. **42**(13), 2431–2434 (2017).
3. F. Druon, F. Balembois, and P. Georges, "New laser crystals for the generation of ultrashort pulses," C. R. Phys. **8**(2), 153–164 (2007).
4. A. Yoshida, A. Schmidt, V. Petrov, C. Fiebig, G. Erbert, J. Liu, H. Zhang, J. Wang, and U. Griebner, "Diode-pumped mode-locked Yb:YCOB laser generating 35 fs pulses," Opt. Lett. **36**(22), 4425–4427 (2011).
5. W. Tian, G. Wang, D. Zhang, J. Zhu, Z. Wang, X. Xu, J. Xu, and Z. Wei, "Sub-40-fs high-power Yb:CALYO laser pumped by single-mode fiber laser," High Power Laser Sci. Eng. **7**, e64 (2019).
6. C. Paradis, N. Modsching, V. J. Wittwer, B. Deppe, C. Kränkel, and T. Südmeyer, "Generation of 35-fs pulses from a Kerr lens mode-locked Yb:$Lu_2O_3$ thin-disk laser," Opt. Express **25**(13), 14918–14925 (2017).
7. F. Pirzio, M. Kemnitzer, A. Guandalini, F. Kienle, S. Veronesi, M. Tonelli, J. Aus der Au, and A. Agnesi, "Ultrafast, solid-state oscillators based on broadband, multisite Yb-doped crystals," Opt. Express **24**(11), 11782–11792 (2016).
8. S. Manjooran and A. Major, "Diode-pumped 45 fs Yb:CALGO laser oscillator with 1.7 MW of peak power," Opt. Lett. **43**(10), 2324–2327 (2018).
9. P. Sévillano, P. Georges, F. Druon, D. Descamps, and E. Cormier, "32-fs Kerr-lens mode-locked Yb:$CaGdAlO_4$ oscillator optically pumped by a bright fiber laser," Opt. Lett. **39**(20), 6001–6004 (2014).
10. H. J. Zeng, Z. L. Lin, W. Z. Xue, G. Zhang, Y. Chen, Z. Pan, V. Petrov, P. Loiko, X. Mateos, Y. Zhao, H. Lin, L. Wang, and W. Chen, "Soliton mode-locked Yb:$Ca_3Gd_2(BO_3)_4$ laser," Opt. Express **30**(7), 11833–11839 (2022).
11. S. Sun, H. J. Zeng, Z. L. Lin, W. Z. Xue, G. Zhang, Z. Lin, V. Petrov, H. Lin, P. Loiko, X. Mateos, Y. Zhao, B. Teng, L. Wang, and W. Chen, "SESAM mode-locked Yb:$Sr_3Y_2(BO_3)_4$ laser," Opt. Express **30**(7), 11861–11871 (2022).
12. H. J. Zeng, Z. L. Lin, W. Z. Xue, G. Zhang, Z. Pan, H. Lin, P. Loiko, X. Mateos, V. Petrov, L. Wang, and W. Chen, "SESAM mode-locked Yb:$SrLaAlO_4$ laser," Opt. Express **29**(26), 43820–43826 (2021).
13. N. Modsching, C. Paradis, F. Labaye, M. Gaponenko, I. J. Graumann, A. Diebold, F. Emaury, V. J. Wittwer, and T. Südmeyer, "Kerr lens mode-locked Yb:CALGO thin-disk laser," Opt. Lett. **43**(4), 879–882 (2018).
14. J. Ma, H. Huang, K. Ning, X. Xu, G. Xie, L. Qian, K. P. Loh, and D. Tang, "Generation of 30 fs pulses from a diode-pumped graphene mode-locked Yb:$CaYAlO_4$ laser," Opt. Lett. **41**(5), 890–893 (2016).
15. S. Kimura, S. Tani, and Y. Kobayashi, "Raman-assisted broadband mode-locked laser," Sci. Rep. **9**(1), 3738 (2019).
16. F. Labaye, V. J. Wittwer, M. Hamrouni, N. Modsching, E. Cormier, and T. Südmeyer, "Efficient few-cycle Yb-doped laser oscillator with Watt-level average power," Opt. Express **30**(2), 2528–2538 (2022).
17. Z. Gao, J. Zhu, Z. Wu, Z. Wei, H. Yu, H. Zhang, and J. Wang, "Tunable second harmonic generation from a Kerr-lens mode-locked Yb:$YCa_4O(BO_3)_3$ femtosecond laser," Chin. Phys. B **26**(4), 044202 (2017).
18. Y. Wang, X. Su, Y. Xie, F. Gao, S. Kumar, Q. Wang, C. Liu, B. Zhang, B. Zhang, and J. He, "17.8 fs broadband Kerr-lens mode-locked Yb:CALGO oscillator," Opt. Lett. **46**(8), 1892–1895 (2021).
19. J. Ma, F. Yang, W. Gao, X. Xiaodong, X. Jun, D. Shen, and D. Tang, "Sub-five-optical-cycle pulse generation from a Kerr-lens mode-locked Yb:$CaYAlO_4$ laser," Opt. Lett. **46**(10), 2328–2331 (2021).
20. S. Uemura and K. Torizuka, "Sub-40-fs pulses from a diode-pumped Kerr-lens mode-locked Yb-doped yttrium aluminum garnet laser," Jpn. J. Appl. Phys. **50**(10), 010201 (2011).
21. J. Drs, J. Fischer, N. Modsching, F. Labaye, V. J. Wittwer, and T. Südmeyer, "Sub-30-fs Yb:YAG thin-disk laser oscillator operating in the strongly self-phase modulation broadened regime," Opt. Express **29**(22), 35929–35937 (2021).
22. U. Keller, D. A. B. Miller, G. D. Boyd, T. H. Chiu, J. F. Ferguson, and M. T. Asom, "Solid-state low-loss intracavity saturable absorber for Nd:YLF lasers: an antiresonant semiconductor Fabry-Perot saturable absorber," Opt. Lett. **17**(7), 505–507 (1992).
23. R. Paschotta and U. Keller, "Passive mode locking with slow saturable absorbers," Appl. Phys. B: Lasers Opt. **73**(7), 653–662 (2001).
24. C. Honninger, R. Paschotta, F. Morier-Genoud, M. Moser, and U. Keller, "Q-switching stability limits of continuous-wave passive mode locking," J. Opt. Soc. Am. B **16**(1), 46–56 (1999).
25. U. Demirbas, J. Thesinga, M. Kellert, S. Reuter, M. Pergament, and F. X. Kärtner, "Semiconductor saturable absorber mirror mode-locked Yb:YLF laser with pulses of 40 fs," Opt. Lett. **47**(4), 933–936 (2022).
26. M. Weber, M. Bass, K. Andringa, R. Monchamp, and E. Comperchio, "Czochralski growth and properties of $YAlO_3$ laser crystals," Appl. Phys. Lett. **15**(10), 342–345 (1969).

Optics EXPRESS


27. R. Diehl and G. Brandt, "Crystal structure refinement of $YAlO_3$, a promising laser material," Mater. Res. Bull. **10**(2), 85–90 (1975).
28. K. W. Martin and L. G. DeShazer, "Indices of refraction of the biaxial crystal $YAlO_3$," Appl. Opt. **12**(5), 941–943 (1973).
29. G. Boulon, Y. Guyot, H. Canibano, S. Hraiech, and A. Yoshikawa, "Characterization and comparison of $Yb^{3+}$-doped $YAlO_3$ perovskite crystals (Yb:YAP) with $Yb^{3+}$-doped $Y_3Al_5O_{12}$ garnet crystals (Yb:YAG) for laser application," J. Opt. Soc. Am. B **25**(5), 884–896 (2008).
30. R. Aggarwal, D. Ripin, J. Ochoa, and T. Fan, "Measurement of thermo-optic properties of $Y_3Al_5O_{12}$, $Lu_3Al_5O_{12}$, $YAIO_3$, $LiYF_4$, $LiLuF_4$, $BaY_2F_8$, $KGd(WO_4)_2$, and $KY(WO_4)_2$ laser crystals in the 80 – 300 K temperature range," J. Appl. Phys. **98**(10), 103514 (2005).
31. K. Hovhannesyan, M. Derdzyan, A. Yeganyan, V. Kisel, A. Rudenkov, N. Kuleshov, and A. Petrosyan, "Single crystals of YAP:Yb for ultra short pulse lasers," Contemp. Phys. **55**(2), 131–136 (2020).
32. J. Petit, B. Viana, P. Goldner, J. P. Roger, and D. Fournier, "Thermomechanical properties of $Yb^{3+}$ doped laser crystals: Experiments and modeling," J. Appl. Phys. **108**(12), 123108 (2010).
33. Y. Song, N. Zong, K. Liu, Z. Wang, X. Wang, Y. Bo, Q. Peng, and Z. Xu, "Temperature-dependent thermal and spectroscopic properties of Yb:$YALO_3$ perovskite crystal for a cryogenically cooled near IR laser," Opt. Mater. Express **10**(7), 1522–1530 (2020).
34. V. E. Kisel, S. V. Kurilchik, A. S. Yasukevich, S. V. Grigoriev, S. A. Smirnova, and N. V. Kuleshov, "Spectroscopy and femtosecond laser performance of $Yb^{3+}$:$YAlO_3$ crystal," Opt. Lett. **33**(19), 2194–2196 (2008).
35. A. Rudenkov, V. Kisel, A. Yasukevich, K. Hovhannesyan, A. Petrosyan, and N. Kuleshov, "High power SESAM mode-locked laser based on $Yb^{3+}$:$YAlO_3$ bulk crystal," Devices Methods Measure. **11**(3), 179–186 (2020).
36. W. Z. Xue, Z. L. Lin, H. J. Zeng, G. Zhang, P. Zhang, Z. Chen, Z. Li, V. Petrov, P. Loiko, X. Mateos, H. Lin, Y. Zhao, L. Wang, and W. Chen, "Diode-pumped SESAM mode-locked Yb:(Y,Gd)$AlO_3$ laser," Opt. Express **30**(7), 11825–11832 (2022).
37. X. He, G. Zhao, X. Xu, X. Zeng, and J. Xu, "Comparison of spectroscopic properties of Yb:YAP and Yb:YAG crystals," Chin. Opt. Lett. **5**(5), 295–297 (2007).
38. X. Zeng, G. Zhao, X. Xu, H. Li, J. Xu, Z. Zhao, X. He, H. Pang, M. Jie, and C. Yan, "Comparison of spectroscopic parameters of 15 at% Yb:$YAlO_3$ and 15 at% Yb:$Y_3Al_5O_{12}$," J. Cryst. Growth **274**(1-2), 106–112 (2005).
39. X. Wang, X. Xu, Z. Zhao, B. Jiang, J. Xu, G. Zhao, P. Deng, G. Bourdet, and J. C. Chanteloup, "Comparison of fluorescence spectra of Yb:$Y_3Al_5O_{12}$ and Yb:$YALO_3$ single crystals," Opt. Mater. **29**(12), 1662–1666 (2007).
40. J. A. Caird, S. A. Payne, P. R. Staver, A. Ramponi, and L. Chase, "Quantum electronic properties of the $Na_3Ga_2Li_3F_{12}$:$Cr^{3+}$ laser," IEEE J. Quantum Electron. **24**(6), 1077–1099 (1988).
41. M. Tokurakawa, A. Shirakawa, K. Ueda, H. Yagi, S. Hosokawa, T. Yanagitani, and A. A. Kaminskii, "Diode-pumped 65 fs Kerr-lens mode-locked $Yb^{3+}$:$Lu_2O_3$ and nondoped $Y_2O_3$ combined ceramic laser," Opt. Lett. **33**(12), 1380–1382 (2008).
42. F. Druon, D. N. Papadopoulos, J. Boudeile, M. Hanna, P. Georges, A. Benayad, P. Camy, J. L. Doualan, V. Menard, and R. Moncorge, "Mode-locked operation of a diode-pumped femtosecond Yb:$SrF_2$ laser," Opt. Lett. **34**(15), 2354–2356 (2009).
43. F. X. Kartner, I. D. Jung, and U. Keller, "Soliton mode-locking with saturable absorbers," IEEE J. Sel. Top. Quantum Electron. **2**(3), 540–556 (1996).